JJMIE

Volume 6, Number 2, April 2012
ISSN 1995-6665
Pages 193 - 198

Jordan Journal of Mechanical and Industrial Engineering

A Sharp-Interface Fluid-Structure Interaction Algorithm for Modeling Red Blood Cells

T. D. AlMomani*[,a], S. C. Vigmostad[b] and L. A. Alzube[a]

[a]*Biomedical Engineering Department, The Hashemite University, P.O. Box 150459, Zarqa 13115, Jordan*
[b]*Biomedical Engineering Department, The University of Lowa, Iowa city, IA, USA 52242*

Abstract

RBC deformation is thought to play a major role in both RBC dynamics and functionality. Due to the difficulty of experiments on real RBCs, researchers tend to perform computational simulations that can cover RBC dynamics and blood rheology. However, modeling of RBC with physiological conditions is still not completely well established. The current work utilized the immersed interface method and implements the fluid structure interaction technique to propose a new computational model of RBC as a biconcave fluid-filled cell. RBC is presented by a two dimensional hyperelastic massless membrane that surrounded by plasma and enclosed hemoglobin. The physiological viscosity ratio for the hemoglobin to that of plasma and their interactions with the cell membrane is considered. Pressure and velocity jump conditions are applied at the membrane, so that the influence of extracellular fluid can be transferred to the intracellular fluid. The model was applied to study the deformation of a single RBC as it flows in straight channels with geometries similar to that could find in capillaries with low Reynolds numbers that vary from 0.001 to 0.01. As Reynolds number increases, RBC shows higher levels of deformation. Flow fields through the cell membrane are appeared to be different and jumps in both velocity and pressure can be clearly seen.

Keywords: Red blood cell; Hyperelastic membrane; Jump conditions; Deformation; Capillaries

1. Introduction

The primary function of red blood cells (RBCs) or erythrocytes is delivering oxygen to different body organs and tissues. RBCs can be defined as nucleus-free deformable liquid capsules enclosed by a biological membrane that is nearly incompressible and exhibits a viscoelastic response to shearing and bending deformation [7]. Many researchers have described RBC as a capsule that consists of an elastic membrane that encloses a concentrated solution of hemoglobin [6]. RBCs are produced from bone marrow at a rate of 2 – 3 million cells per second, and have a lifespan of roughly 120 days. Adult humans have about 2–3 × 10^{13} red blood cells that circulate around their cardiovascular system. Hematocrit is defined as the volume percentage of RBCs in the whole blood; it's about 47% for adult men, and 43% for the adult women. RBCs have a distinctive biconcave shape, with 8μm diameter and 2 μm thickness. This shape gives RBCs a larger surface area, about 47% higher than a sphere of the same volume [3]. Additionally, this shape gives RBC the ability to exhibit high levels of deformation as it exposed to blood forces or flow in small diameter capillaries. Secomb 2003 has reported that RBCs can be folded and flow through a capillary with a diameter as small as 2.8 μm [17].

To date, many studies (both experimental and numerical) have been accomplished on RBC dynamics and their interaction with blood plasma, other blood constituents, vessel walls, and medical implants. The motivation of these studies would be among one of the following main reasons:

- At the microcirculatory level, the particulate nature of the RBC becomes important in determining blood properties and behavior, such as viscosity and non-Newtonian nature of the blood.
- Studying the biconcave shape of healthy RBCs helps in assessing cell membrane stress state .
- RBCs are proposed to have a major role in many cardiovascular diseases such as thrombosis (platelet activation) and atherosclerosis.

The small size, and high sensitivity to external conditions makes it difficult to perform *in vivo* experimentations on RBCs and other blood particles. Consequently, researchers tend to design experiments with single RBCs and employed simplified flow conditions [11]. Also due to these challenges, researchers took advantage of various numerical techniques to study the behavior of RBCs under different flow conditions and circumstances. They used different numerical methods such as finite element, immersed boundary, and boundary element techniques which can capture the deformation of

* Corresponding author. e-mail: thakir2000@hu.edu.jo

RBCs in different flow environments [11]. However, these numerical simulations have invoked significant assumptions in modeling the RBCs that are not physiologically correct [6].

Over the past few decades efforts to describe the micromechanics of the RBCs have led to several mathematical and computational models, the most popular RBC models are:

- Modeling RBCs as elliptical non-deformable particles [1].
- Modeling RBCs as elliptical deformable particles [10, 17].
- Modeling RBCs as fluid bubbles that resist flow by surface tension [25].
- Modeling RBCs as biconcave, assuming that the membrane is an elastic material that resists shearing, bending, or both [16].
- Modeling RBCs as biconcave, assuming that the membrane is a viscoelastic material that resists shearing and bending [4, 5].

The current work proposes a new model of the RBC as a biconcave, fluid-filled cell. This model considers a physiologically realistic viscosity ratio for the RBC intracellular fluid (primarily hemoglobin) to that of outer cellular fluid (or blood plasma) and the interactions with the cell membrane. Furthermore, RBCs are treated using an immersed interface approach similar to the one described in Lai and Li 2001 and Vigmostad et al. 2009 [12, 23].

The RBC membrane was modeled as a hyperelastic, massless membrane that separate two fluids, blood plasma outside and hemoglobin inside [2]. Membrane deformation was computed based on fluid forces on both sides of the membrane, where velocity and pressure jump conditions are imposed on the fluid based on the calculated membrane stresses.

2. Computational Approach

2.1. Governing Equation:

Continuity and momentum equations of incompressible flow with constant density were solved. The non-dimensionlized forms of these equations are given by:

$$\nabla \cdot \mathbf{u} = 0 \tag{1}$$

$$\frac{\partial \mathbf{u}}{\partial t} + \mathbf{u} \cdot \nabla \mathbf{u} = -\nabla p + \frac{1}{\mathrm{Re}} \nabla^2 \mathbf{u} + \mathbf{F} \tag{2}$$

Where $\mathrm{Re} = \rho_0 \mathbf{U}_0 D / \mu$, denotes the Reynolds number, $\mathbf{F}$ is a term that represent a singular force at the RBC membrane (this term will discuss later in details). The following variables are used as non-dimensionalzing groups:

$$\mathbf{u} = \frac{\mathbf{u}^*}{\mathbf{U}_0},\ L = \frac{L^*}{D_0},\ P = \frac{P^*}{\rho \mathbf{U}_0^2}$$

Where, $\mathbf{u}$ is the dimensional velocity field, $\mathbf{U}_0$ is the average axial velocity at the inlet, r_0 and m are the density and viscosity, and P^* is the dimensional pressure. The inlet gap width is denoted by D_0, and the characteristic pressure is $r_0 U_0^2$.

2.2. Flow solver and implicit representation of RBC:

The governing equations are discretized using a cell-centered collocated-variable semi-implicit approach. The solution is then advanced in time using the two-step fractional step method [24]. The embedded RBC is presented in the flow solver by using a sharp-interface method as used before in AlMomani et al 2008, Marella 2005, Marella and Udaykumar 2004 [1, 13, 14]. RBCs are represented implicitly on the mesh using a level-set approach [18, 19, 20]. The level-set (representing an embedded boundary – here an RBC) is represented by a scalar field denoted by ϕ_l, where l represents the l_{th} embedded interface or RBC. The normal distance from the l_{th} embedded interface at any point is representative of the value of ϕ_l. Values of ϕ_l less than zero (ϕ_l <0) represent the inside of the RBC, values of ϕ_l greater than zero (ϕ_l > 0) represent the outside of the RBC, the boundary (the membrane) of the RBC is presented by the zero ϕ_l values (i.e. ϕ_l = 0). Motion and deformation of the interface is computed based on the flow field and tracked using Lagrangian points describing the interface boundary, and employed to compute the RBC deformation.

2.3. Fluid structure interaction:

Fluid structure interaction (FSI) technique involves solving flow interacting with immersed structures. Generally, there are two FSI approaches that can be employed by the flow solver currently in use: The first approach is that in which the embedded object is treated as an immersed interface as described in Lai and Li 2001 and further outlined in Vigmostad et al. 2009 [12, 23]. Here, the assumption is that the surrounding is a massless membrane interface contributes singular stress fields [23]. In this approach the viscosity inside and outside of the membrane can be different, as is appropriate in the case of an RBC. The second approach is that which the embedded object is treated as a solid object that deforms as a result of the surrounding fluid forces. In this case, no-slip and no-penetration are used as boundary conditions on the solid surface [22]. The current work will utilize the first approach or FSI approach 1 to propose a new model of RBC as it expose to fluid forces.

2.3.1. Modeling of RBC using of FSI approach:

Here RBC is modeled as a hyperelastic massless membrane that separate two fluids, blood plasma outside and hemoglobin inside. The displacement and the deformation of this membrane are computed based on the fluid forces acting on this membrane as shown in Figure 1.

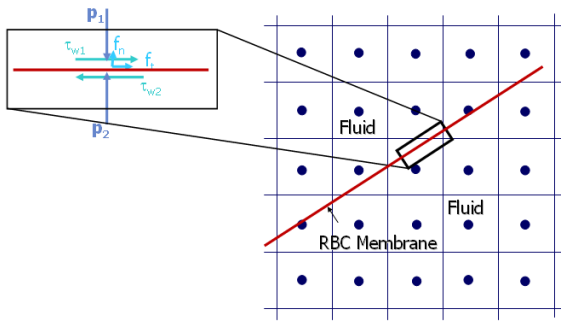

Figure 1: Force balance represented by a fluid-fluid interface separated by a membrane.

2.3.2. Approach to jump conditions using delta function:

Initially the singular force at the interface is presented by a delta function **f**, such that [12]:

$$\mathbf{f}(\mathbf{x},t)=\int_{\sigma}\mathbf{F}(r,s,t)\delta(\mathbf{x}-\mathbf{X}(r,s,t))drds \tag{3}$$

Where $\mathbf{f}(\mathbf{x},t)$ is the force density exerted by the membrane, and the membrane σ is represented by $\mathbf{X}(r,s,t)$ where *r*, *s* are parameters of a reference configuration where $0\le r\le L_r$ and $0\le s\le L_s$. The Dirac delta function is three-dimensional, and the membrane force, $\mathbf{F}(r,s,t)$ is a function of its configuration, where $\mathbf{F}(r,s,t)=\mathbf{S}(\mathbf{X}(r,s,t),t)$.

In other words, at any time, *t*, a region on the surface of the membrane is mapped onto a patch with area $L_r\times L_s$ and all calculations are performed in this reference space [22].

These calculations could also be performed in the current space, with $\mathbf{F}(\sigma,t)$ instead of mapping it back to a reference configuration. In this way, the above equation would change to:

$$\mathbf{f}(\mathbf{x},t)=\int_{\sigma}\mathbf{F}(l,m,t)\delta(\mathbf{x}-\mathbf{X}(\sigma,t))dldm \tag{4}$$

Where *l*, *m* are parameterized curves acting in the two *local* tangent directions, τ_1,τ_2. Consequently, by introducing the force f as a source term to the momentum equation, the governing equations of the fluid became as:

$$\nabla\cdot\mathbf{u}=0 \tag{5}$$

$$\frac{\partial\mathbf{u}}{\partial t}+\mathbf{u}\cdot\nabla\mathbf{u}=-\nabla p+\frac{1}{\mathrm{Re}}\nabla^2\mathbf{u}+\mathbf{f} \tag{6}$$

A summary of the jumps in pressure and velocities, and their derivatives, in the normal and two tangential directions are shown below:

- $[u]=[v]=[w]=0$ (from continuity/no-slip)
- $\left[u_x+v_y+w_z\right]=0$ (from incompressibility)
- $\left[\frac{\partial\mathbf{u}}{\partial\mathbf{n}}\right]\cdot\mathbf{n}=0$ (from incompressibility + continuity)
- $\left[\mathbf{u}_t\right]+\left[\nabla\mathbf{u}\right]\cdot\mathbf{u}=\mathbf{0}$ (from incompressibility)
- $[\nabla u\cdot\tau_1]=[\nabla v\cdot\tau_1]=[\nabla w\cdot\tau_1]=0$ (from continuity)
- $[\nabla u\cdot\tau_2]=[\nabla v\cdot\tau_2]=[\nabla w\cdot\tau_2]=0$ (from continuity)
- $[p]=[m]\frac{\partial\mathbf{u}}{\partial\mathbf{n}}\cdot\mathbf{n}+\mathbf{F}\cdot\mathbf{n}$
- $\left[\mu\frac{\partial\mathbf{u}}{\partial\mathbf{n}}\right]=[\mu]\left(\frac{\partial\hat{\mathbf{u}}}{\partial\mathbf{n}}\cdot\mathbf{n}\right)\mathbf{n}+(\mathbf{F}\cdot\mathbf{n})\mathbf{n}-\mathbf{F}$
- $\left[\frac{\partial p}{\partial\mathbf{n}}\right]=\frac{\partial}{\partial\boldsymbol{\tau}_1}\mathbf{F}\cdot\boldsymbol{\tau}_1+\frac{\partial}{\partial\boldsymbol{\tau}_2}\mathbf{F}\cdot\boldsymbol{\tau}_2$
- $\left[\frac{\partial p}{\partial\boldsymbol{\tau}_1}\right]=\frac{\partial}{\partial\boldsymbol{\tau}_1}\left([\mu]\left(\frac{\partial\hat{\mathbf{u}}}{\partial\mathbf{n}}\cdot\mathbf{n}\right)+(\mathbf{F}\cdot\mathbf{n})\right)$
- $\left[\frac{\partial p}{\partial\boldsymbol{\tau}_2}\right]=\frac{\partial}{\partial\boldsymbol{\tau}_2}\left([\mu]\left(\frac{\partial\hat{\mathbf{u}}}{\partial\mathbf{n}}\cdot\mathbf{n}\right)+(\mathbf{F}\cdot\mathbf{n})\right)$

Finally the FSI algorithm in approach 1 can be summarized in the following main steps:

For any new time step (n+1):

A. Compute the intermediate velocity, $\vec{\mathbf{u}}_f^{\,*n+1}$

B. Iterate until pressure and stress are converged, iteration (k+1):

- Solve for $p^{n+1,k+1}$
- Correct velocity, such that $\vec{u}_f{}^{n+1,k+1}$
- move interface, $\vec{u}_s{}^{n+1,k+1}=\vec{u}_f{}^{n+1,k+1}$
- compute interface stresses $\sigma^{n+1,k+1}$

3. Computational Results

The above algorithm has been applied to investigate the deformation of a single RBC as it flows in a microchannel with flow conditions similar to what can be found in capillaries. A straight tube with diameter of 12 μm (equivalent to 1.5 RBC major diameters) and length of 120 μm was used. Reynolds numbers of 0.001, 0.002, 0.004, and 0.01 were used in the current computations. Initially, the two dimensional (2D) unstressed biconcave shape of RBC, shown in Figure 2, is assumed. This shape is described by the following parametric equations [15]:

$$y=a\frac{\alpha}{2}(0.207+2.003\sin^2\chi-1.123\sin^4\chi)\cos\chi,\qquad x=a\alpha\sin \tag{10}$$

Where, a is the equivalent cell radius and equal to 2.8 μm, α = 1.38581894 is the ratio between the maximum radius of the biconcave disk (b in Figure 2), and the equivalent radius a, and finally, the parameter χ ranges from -π/2 to π/2.

  - Volume 6, Number 2 (ISSN 1995-6665)

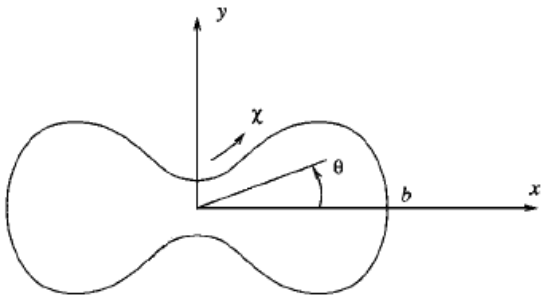

Figure 2: Biconcave shape of RBC.

3.1. Boundary and initial conditions:

At the inlet, the following parabolic velocity profile was used,

$$\mathbf{u}(y) = 4\mathbf{u}_{\max}(d_i y - y^2)/d_i^2 \quad (11)$$

Where u(y) is the velocity at y-location, u_{max} is the maximum inlet velocity, and di is the inlet diameter of the geometry. At the outlet, the velocities were linearly extrapolated and corrected to be consistent with global mass conservation and a Neumann condition was applied on the pressure [13, 14]. Finally, a no-slip (or wall) boundary condition was applied on the top and the bottom of the geometry.

3.2. Physiological assumptions:

In the current computations, the plasma (the external fluid) is assumed to behave as a Newtonian homogenous fluid, with a viscosity coefficient of 1.2 cP and the internal fluid is hemoglobin which was treated as a homogenous Newtonian fluid, as well, with a viscosity coefficient that is equivalent to five times the plasma viscosity (i.e. 6 cP). It is also assumed that only viscous and inertial forces affect the deformation of the RBC membrane and the effect of gravity is neglected. RBC is initially arranged in a vertical position in which the major axis of the RBC is parallel to the y-axis (90 degrees). The computations were performed for enough time so steady state of RBC deformation is reached as show in the result section.

3.3. Deformation of single RBC:

The biconcave shape of the RBC is initially assumed as stress free shape; i.e. the membrane is initially constructed such that no stresses and no strains can be found in this membrane. The fluid and membrane are fully coupled, so that the stress in the membrane affects the fluid as well as the fluid motion and forces affect the membrane behavior and deformation. Since the membrane moves with the fluid velocity, then no-slip is enforced at the interface implicitly. Membrane stress is computed assuming a hyperelastic material model as:

$$\boldsymbol{\sigma} = \mu\,(\mathbf{F}\mathbf{F}^T - \mathbf{I}) \quad (12)$$

Where, F is the deformation gradient, $\boldsymbol{\sigma}$ is the Cauchy stress, and μ is the Neo-Hookean elastic modulus, in the current computation a value of 0.005 dyn/cm is used [21].

The deformation profiles of a single RBC for Reynolds number values of 0.001, 0.002, 0.004, and 0.01 are presented in figure 3. The short axis of the RBC was coincided along the central axis of the capillary (or the straight tube). In all cases, RBC undergoes different levels of deformations. For Re = 0.001 (figure 3.a), RBC showed slight deformation and reached a steady state shape (starting at x = 5) allowing the deformed shape to be maintained as the RBC moves through the channel. Higher deformation levels are observed by increasing the Reynolds number (Figure 3: b, c, and d).

Finally, and for all Reynolds numbers, the RBC appeared to fold (with different degrees) in response to the fluid forces and reach the steady state shape while it moves with the fluid across the channel. As the Reynolds number increases (i.e. higher inertia forces), RBC folds more. In the case of Re =0.01, the steady state deformed shape of the RBC was more like a parachute shape.

3.4. Flow fields:

Figures 3 shows the velocity contours of flow at different time step for a Re = 0.001, Re = 0.002, Re = 0.004, and Re =0.01 respectively. This figure is also showing different deformation profiles of a single RBC as it exposed to a channel flow conditions, with flow values close enough or similar to the flow conditions that could find in the capillaries. RBC appeared to have major influence on both velocity and pressure fields. As can be observed in figure 4, that represent the pressure and velocity contours for deformed RBC with Re = 0.001, both velocity and pressure contours seem to jump at the area of the RBC membrane, also the pressure and velocity contours inside the RBC seem to be different form those out of the RBC. However, no discontinuity is observed between the two flow fields. This agrees with the idea of jump conditions which aims at transferring the influence of the outer fluid to the inner fluid through the RBC membrane without discontinuity. On the other hand, the differences between the two flow fields can be explained by the fact that these two fields have two different fluids with different viscosity values, which means that fluid forces are expected to be different in these two regions. Furthermore, the membrane of the RBC is expected to have a major contribution in the flow field through the membrane forces (or tension) that are applied to the fluids through the membrane forces or **F** term that imposed in the momentum equation.

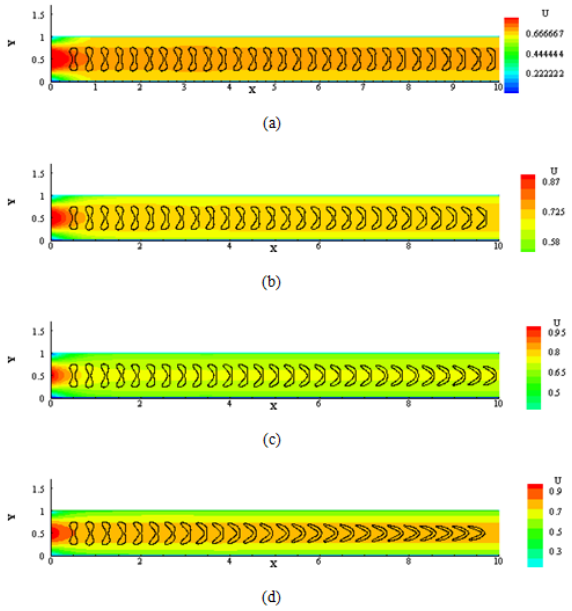

Figure 3: Velocity contours and the deformation profile of a single RBC as it flows through a straight channel with: a) Re = 0.001, b) Re = 0.002, c) Re = 0.004, d) Re = 0.01.

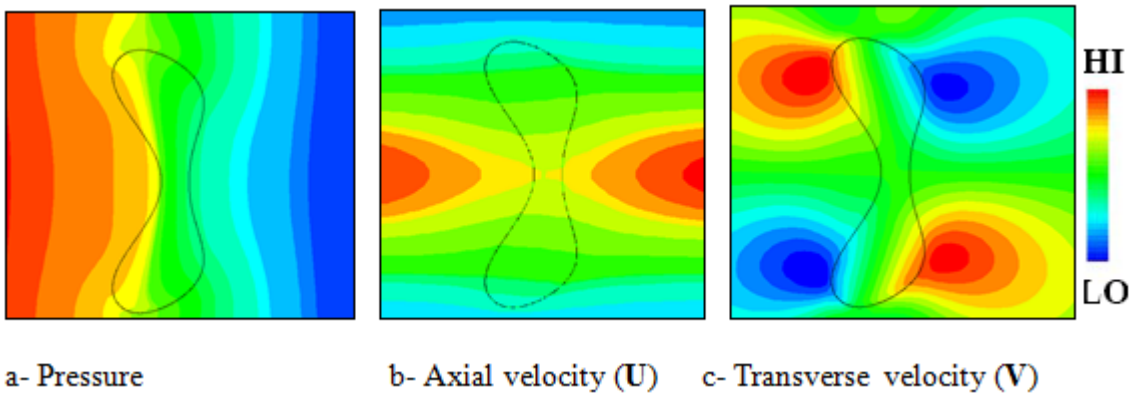

Figure 4: Pressure, axial velocity, and transverse velocity contours in the focused in the region surrounding a single RBC. Applied Reynolds number = 0.001.

4. Discussion and Conclusion

A fluid-structure interaction (FSI) algorithm has been developed and used to study the behavior of deformable RBC as it flow in a microchannel with dimensions similar to that could find in capillaries. In this algorithm, RBC was presented as a biconcave, hyperelastic, massless membrane that enclosed a Newtonian fluid (representing hemoglobin). Two-dimensional simulations are used to study the effect of intracellular and extracellular fluids on the cell membrane. Physiological viscosity values of plasma (or extracellular fluid) and hemoglobin (intracellular fluid) are used in the current computations. The membrane was modeled as a Neo-hookean elastic material that deform as a result of net fluid forces acting on the membrane from both inner and outer sides. Pressure and velocity jump conditions are applied to transfer the influence of the external fluid through the membrane to the internal fluid.

Reynolds number was defined based on the average axial flow velocity and using the diameter of the microchannel. At low Reynolds number of 0.001, RBC showed negligible deformation and it kept its un-deformed biconcave shape (Figure 3.a). This behavior changed as the Reynolds number increased resulting in higher levels of deformation. In all cases, RBC appeared to take a butterfly shape and fold more as the fluid inertia forces increases (higher Reynolds number) (Figure 3.b, c, and d). Furthermore, velocity and pressure contours were plotted to inspect the influence of the used jump conditions on both the extracellular and intracellular flows (Figure 4). Pressure and velocity contours seemed to change critically across the cell membrane. This change can be observed through the changes in the contour levels and gradients. Still, no discontinuity was observed between both sides of the membrane, which can be explained due to the use of proper pressure and velocity jump conditions. As mentioned earlier, the objective of using jump conditions is to transfer the influence and changes happening in the extracellular flow to the intercellular flow through the interaction and the deformation of the cell membrane. In

the current approach, this goal has been achieved through the application of the membrane forces as a source term in the Navier-Stokes equations. This source term reflects the interaction between the elastic nature of the membrane itself and both intracellular and extracellular flow regimes.

In conclusion, this work proposed a new technique to simulate physiological behavior of RBC using simplified flow condition. The agreement between the results of the current study and those found in the previous experimental and numerical studies improve that the new approach can be easily expanded to more realistic physiological flow conditions. Computations handle larger numbers of RBCs in the same domain as well as higher Reynold's numbers are being currently investigated. These computations will include the interaction of deformable RBCs with other blood cells, artificial walls, and vessel walls. Furthermore, the current computations will be extended to involve 3D simulations of single and multi RBCs.

References

[1] AlMomani T, UdayKumar S H, Marshall J, Krishnan B C (2008) Micro-scale dynamics of erythrocytes-platelet interaction in blood flow. Annals of Biomedical Engineering 36 (6): 905-920.

[2] AlMomani T, Vigmostad S, UdayKumar S, Krishnan B C (2010) Modeling of red blood cell dynamics using fluid structure interface (FSI) technique. Proceedings of ASME 2010 Summer Bioengineering Conference. FL, USA, June, 2010.

[3] Chandran KB, Rittgers SE, Yoganathan AP (2007) Biofluid Mechanics: The Human Circulation. CRC/Taylor & Francis: Boca Raton, 2007; 419.

[4] Chang K S and Olbrecht W L (1993) Experimental studies of the deformation of a synthetic capsule in extensional flow. J. Fluid Mech. 250: 587-993.

[5] Chang K.S. and Olbrecht W L (1993) Experimental studies of the deformation and breakup of a synthetic capsule in steady and unsteady simple shear flow. J. Fluid Mech. 250: 609-1993.

[6] Cristini, V and Kassab G S (2005) Computer modeling of red blood cell rheology in the microcirculation: a brief overview. Annals of Biomedical Engineering. 33(12): 1724–1727.

[7] Eggleton, C D and Popel A S (1998) Large deformation of red blood cell ghosts in a simple shear flow. Phys. Fluids. 10: 1834–1845.

[8] Fishcer T M, Cees W M, Haest Stohr-Liesen M, and Schmid-schobein H (1981) The stress-free shape of the red blood cell membrane. Biophys. J. 34: 409 – 422.

[9] Gong X, Sugiyama K, Takagi S, and Matsumoto Y (2009) The Deformation Behavior of Multiple Red Blood Cells in a Capillary Vessel. J. of Biomechanical Engineering. 131: 074504-074511.

[10] Keller Stuart R and Skalak Richard (1982) Motion of a tank-treading ellipsoidal particle in a shear flow. J. Fluid Mech.. 120: 27-47.

[11] Korin N, Bransky A, and Uri Dinnar (2007) Theoretical model and experimental study of red blood cell (RBC) deformation in microchannels. Journal of Biomechanics. 40: 2088–2095.

[12] Lai, M C, and Li Z (2001) A Remark on Jump Conditions for the Three-Dimensional Navier-Stokes Equations Involving an Immersed Moving Membrane, Applied Mathematics Letters. 14: 149-154.

[13] Marella S, Krishnan S, Liu H, Udaykumar HS (2005) Sharp interface cartesian grid method I: an easily implemented technique for 3D moving boundary computations. Journal of Computational Physics. 210(1):1-31.

[14] Marella S., and Udaykumar H (2005) Computational analysis of the deformability of leukocytes modeled with viscous and elastic structural components. Phys. Fluids. 16: 244–264.

[15] Pozrikidis C (2003) Numerical simulation of the flow-induced deformation of red blood cells. Annals of Biomedical Engineering. 31: 1194–1205.

[16] Pozrikidis C (2001) Effect of membrane bending stiffness on the deformation of capsules in simple shear flow. J. Fluid Mech. 440: 269-291.

[17] Secomb T W (2003) Mechanics of red blood cells and blood flow in narrow tubes', In: C. Pozrikidis, ed. Modeling and Simulation of Capsules and Biological Cells. CRC Mathematical Biology and Medicine Series, Chapman & Hall, Boca Raton. 163–190.

[18] Sethian, J A (2001) Evolution, implementation, and application of levelset and fast marching methods for advancing fronts. J. Comp. Phys. 169:503–555.

[19] Sussman M. and Fatemi E (1999). An efficient, interface-preserving levelset redistancing algorithm and its applications to interface incompressible fluid flow. SIAM J. Sci. Comput. 20:1165–1191.

[20] Sussman M, Fatemi E, Smereka P, and Osher S (1998) An improved levelset methods for incompressible two-phase flows. Comput. Fluids. 27:663–680.

[21] Takagi S, Yamada T, Gong X, and Matsumoto Y (2009) The Deformation of a Vesicle in a Linear Shear Flow. Journal of Applied Mechanics. 76:021207

[22] Vigmostad S (2008) A sharp interface fluid-structure interaction model for bioprosthetic heart valve dynamics, University of Iowa, PhD thesis.

[23] Vigmostad S, Udaykumar S, Lu J, and Chandran K B (2009) Fluid–structure interaction methods in biological flows with special emphasis on heart valve dynamics. International Journal for Numerical Method in Biomedical Engineering, 26: 435 – 470.

[24] Zang Y, Street R L, and Koseff J R (1994) A non-staggered grid, fractional step method for time dependent incompressible Navier–Stokes equations in curvilinear coordinates. J. Comp. Phys. 114:18–33.

[25] Zhou H and Pozrikidis C (1995) Deformation of liquid capsules with incompressible interfaces in simple shear flow. Journal of Fluid Mechanics. 283: 175–200.